Biochimica et Biophysica Acta, 1146 (1993) 247–257

BBAMEM 75902

Curvature dependent induction of the interdigitated gel phase in DPPC vesicles

L.T. Boni [a], S.R. Minchey [a], W.R. Perkins [a], P.L. Ahl [a], J.L. Slater [a], M.W. Tate [b], S.M. Gruner [b] and A.S. Janoff [a]

[a] *The Liposome Company, Inc., Princeton, NJ (USA) and* [b] *Department of Physics, Joseph Henry Laboratories, Princeton University, Princeton, NJ (USA)*

(Received 1 September 1992)

Key words: Phospholipid vesicle; Liposome; Captured volume; Ethanol

Ethanol causes biphasic melting behavior in saturated lecithins (Rowe (1983) Biochemistry 22, 3299–3305), a consequence of the formation of the stable interdigitated phase (Simon, S.A. and McIntosh, T.J. (1984) Biochim. Biophys. Acta 773, 169–172). The membrane systems studied to date have been large vesicle systems in which the membrane surface can be assumed to be locally planar. An immediate question arises as to whether surfaces of higher curvature interdigitate. To address this question we have prepared DPPC vesicles of varying diameters which we employed to determine the limiting size at which interdigitation occurs using ethanol as the inducer. We find that with decreasing vesicle size the concentration of ethanol necessary for the onset of interdigitation increases. Small isolated vesicles, at inducing concentrations of ethanol, do not stably interdigitate but rupture and coalesce into a viscous gel comprised of interdigitated lipid sheets. As discussed elsewhere (Ahl et al. (1992) Biophys. J. 243a) these sheets can be used as precursors for producing liposomes of large size and high internal volumes useful in drug delivery or modeling applications.

Introduction

The ability of lipids to coexist in different phases and to undergo transitions between phases is of biophysical and biological importance. Recently attention has been focused on membranes in which the acyl chains of the opposing leaflets become either partially or fully interdigitated depending on acyl chain asymmetry or the presence of inducers [1]. Inducers are amphipathic molecules that localize at the interfacial region of the membrane, presumably displacing head group bound water while partially penetrating into the hydrocarbon core. Examples of lipids that interdigitate in the presence of inducers are saturated symmetric phosphatidylcholines in the presence of ethanol [2], glycerol, methanol, ethylene glycol, benzyl alcohol, chlorpromazine, tetracaine [3,4] or thiocyanate ions [5] and saturated symmetric phosphatidylglycerols in the presence of tris [6] or polymixin B or myelin basic protein [7,8]. Phosphatidylcholines possessing asymmetric acyl chains [9–12] or ether linked acyl chains, such as DHPC [13], interdigitate without inducers. Lyso PCs [14,15] and asymmetric *N*-acylsphingomyelins [16,17] also interdigitate without inducers.

All the membrane systems studied to date have been large vesicles in which the membrane surface can be considered to be locally nearly planar. Here, we investigate whether surfaces of higher curvature interdigitate. Using DPPC liposomes we have determined the limiting size necessary for the induction of interdigitation by ethanol. We find, as described in a preliminary report [18], that with decreasing vesicle size the concentration of ethanol necessary for the onset of interdigitation increases. Small vesicles at and above ethanol concentrations required to induce interdigitation rupture and coalesce into a viscous gel comprised of interdigitated lipid sheets. The principal purpose of this article is to describe the size dependence of the gel to interdigitated gel transition in DPPC systems and characterize the formation of the interdigitated lipid sheets. Elsewhere we describe the use of these sheets

Correspondence to: A.S. Janoff, The Liposome Company, Inc., One Research Way, Princeton, NJ, USA.

Abbreviations: DPPC, dipalmitoylphosphatidylcholine; ANTS, 1-aminonaphthalene-3,6,8,-trisulfonic acid; DPH, 1,6-diphenyl-1,3,5-hexatriene; DPX, *p*-xylyenebis(pyridinium bromide); EPC, egg phosphatidylcholine; NBD-PE, *N*-(7-nitrobenz-2-oxa-1,3-diazol-4-yl)phosphatidylethanolamine; PE, phosphatidylethanolamine; DHPC, dihexadecylphosphatidylcholine; SUV, small unilamellar vesicle; MLV, multilamellar vesicle.

as precursors for the production of liposomes of high captured volumes [19].

Materials and Methods

Chemicals

DPPC, NBD-PE, Rhodamine PE and egg PC were purchased from Avanti Polar Lipids (Alabaster, AL). DPX, ANTS, and DPH were obtained from Molecular Probes (Eugene, OR). Ethanol (dehydrated 200 proof) was obtained from Pharmco (NJ).

Vesicle preparation

MLVS were prepared by drying 100 mg of lipid from chloroform on a rotoevaporator, followed by hydration with 2 ml of 10 mM Tris, 150 mM NaCl (pH 7.4) at 55°C with rigorous vortexing. For the fluorescence interdigitation assay DPH was added to the lipid in chloroform such that the final lipid/DPH mole ratio was 500:1. For the resonance energy transfer experiments both NBD-PE and Rhodamine PE were added such that the final mole percents were 0.35 and 0.65, respectively.

The MLVS were size reduced employing an Extruder (Lipex, Vancouver, BC, Canada). Large unilamellar vesicles by extrusion (LUVETs) were formed by passing the MLVS ten times through double stacked 0.4, 0.2, 0.1, and 0.05 micron polycarbonate filters (Nucleopore, CA). SUVs were prepared by sonicating MLVS in a water bath ultrasonicator (Laboratory Supplies, Hicksville, NY) at 50°C until clear, followed by centrifugation at $10\,000 \times g$ to remove any large vesicles. Liposomes were sized by freeze-fracture electron microscopy using the method of Weibel and Bolender [20].

Fluorescence spectroscopy

Fluorescence measurements were performed on Photon Technology International spectrometers (Princeton, NJ) equipped with water jackets, which were typically equilibrated at 23°C. The DPH assay for monitoring interdigitation of lipids was that of Nambi et al. [21]. For this assay, lipid concentrations were typically varied from 0.15 to 50 mM and were diluted to 0.15 mM prior to measurement. Polystyrene cuvettes (Sarstedt, Princeton, NJ) were employed which allowed over 90% transmission of signal. Scattering intensities from liposomes without probe were less than 0.5% of the respective fluorescence intensities and were subtracted by spectral analysis. The excitation wavelength was 351 nm with the emission spectra measured from 380 to 580 nm and quantitated by cutting and weighing. A pseudo-Stern-Volmer plot of the ratio of F_o/F (F_o is the fluorescence intensity in the absence of ethanol and F is the value in the presence of ethanol) versus the ethanol concentration was employed to determine the quenching attributed to interdigitation. Comparative values of F_o for different vesicle sizes were determined in separate experiments by normalizing the fluorescence obtained in buffer with that obtained when dissolved in 100% ethanol.

Resonance Energy Transfer (RET) measurements were performed to determine the degree of lipid mixing. Vesicles containing both NBD-PE and Rhodamine PE as described above were mixed with blank vesicles at a 1:10 ratio. Excitation was at 465 nm with the emission spectra recorded at 480 to 680 nm. Probe mixing with blank vesicles results in a loss of RET from the NBD moiety to the rhodamine moiety. A standard curve was generated by preparing vesicles of 0.35 mol% NBD-PE and 0.65 mol% Rhodamine PE and sequentially decreasing these concentrations 100-fold to 0.035 and 0.065 to simulate 100% mixing. A direct comparison between the 1:10 mixing experiments in ethanol and this standard curve was used to determine the degree of lipid mixing.

The ANTS/DPX fusion and leakage assay employed was that of Ellens et al. [22]. Liposomes were prepared containing either (a) 25 mM ANTS and 45 mM NaCl, (b) 90 mM DPX or (c) 12.5 mM ANTS, 45 mM DPX and 22.5 mM NaCl. Excitation was at 360 nm and emission was detected at wavelengths greater than 530 nm employing a cutoff filter. Fusion was detected by the mixing of the aqueous contents of ANTS- and DPX-containing liposome (brought together in a 1:9 ratio) by taking advantage of the fact that ANTS fluorescence is quenched in a concentration dependent fashion by DPX. Quantitation of fusion was established by constructing a standard curve in a liposome free system as has been previously described [22]. Leakage was quantitated in separate experiments by monitoring increases in fluorescence upon incubation of vesicles containing both ANTS and DPX in the presence of ethanol. Zero leakage was taken as the fluorescence intensity arising from vesicles in the absence of ethanol and 100% leakage was taken as the fluorescence intensity arising from vesicles lysed by exposure to 1% octyl glucoside (final concentration).

Electron microscopy

For freeze-fracture microscopy, typically a 0.1–0.3 μl aliquot of sample was sandwiched between a pair of Balzers copper support plates (Nashua, NH) and rapidly plunged from 20°C into liquid propane. Samples were fractured and replicated on a Balzers BAF 400 freeze-fracture unit at a vacuum of $4 \cdot 10^{-7}$ mbar or better at -115°C. Replicas were floated off in 3 M HNO_3, and washed in a graded series of Clorox solutions (from 0% to 100%).

For negative staining a drop of specimen was placed on a Formvar-carbon coated grid for one minute and removed with filter paper prior to the application of a

2% ammonium molybdate stain for 30 seconds. Following removal of stain the grids were air dried.

Samples were viewed in a Philips 300 electron microscope at magnifications of 6000 to 27000 ×.

X-ray diffraction

X-ray diffraction intensity versus scattering angle was obtained using a two-dimensional image intensified X-ray detector [23]. Cu K alpha X-rays were generated using a Rigaku RU-200 rotating anode X-ray machine with microfocus cup and were focused via a Franks mirror. Samples were sealed in thin walled glass X-ray capillaries (Charles Supper, Natick, MA) and placed in a thermoelectrically controlled temperature stage (±0.5°C). The resulting two-dimensional powder diffraction images were azimuthally integrated along an arc ±10° from the meridional axis [24]. Long spacings are calibrated against lead stearate (d = 47.5 Å) and the wide angle spacings with p-bromobenzoic acid (d = 14.52 Å). All experiments were performed at 25.0°C.

Results

Freeze fracture electron microscopy was used to determine the size distributions of the liposomes employed in this study. MLVS were quite heterogeneous, typically between 100 and 5000 nm in diameter, LUVETs extruded through 400 nm pore size filters were between 100–430 nm in diameter and were multilamellar. The smaller size reduced vesicles had a more homogeneous size distribution. The 200 nm extruded LUVETs had a mean diameter of 180 nm, the 100 nm extruded LUVETs a mean diameter of 100 nm, the 50 nm extruded LUVETs a mean diameter of 70 nm and the SUVs a mean diameter of 30 nm. Negative stain electron microscopy of the 100 nm and 50 nm extruded LUVETs and the SUVs confirmed the unilamellar nature of these vesicles.

To investigate interdigitation as a function of vesicle size we employed the fluorescence method of Nambi et al. [21], who found that the intensity of DPH incorporated into DPPC MLVS was reduced sequentially by over 50% as these systems underwent a bilayer to interdigitated bilayer transition upon exposure to increasing concentrations of ethanol. They related the cause of these systematic decreases in fluorescence, which could be represented as a sigmoidal shaped quench curve (see Fig. 2, inset), to reorientations of the probe reflecting the membrane phase change. In applying this assay to our investigations we found that the fluorescence intensity of DPH was also systematically affected by vesicle size (Fig. 1). Thus for our purposes, although decreases in DPH fluorescent intensity could be used to detect the onset of the bilayer to interdigitated bilayer phase transition, the magnitude of these changes could not be used to quantitate the extent of interdigitation when comparing vesicle populations of differing sizes. Fig. 2 shows the concentrations of ethanol required to produce the onset of interdigitation in DPPC systems of varying sizes. These values were obtained by fitting the slopes of the sigmoidal quenching curves derived for each vesicle population with straight lines and determining the concentrations of ethanol corresponding to the initial inflections (see figure inset). The ethanol concentration required to induce the onset of interdigitation in SUVs was 1.25 M which was appreciably higher than that concentration needed to first induce interdigitation in MLVs (0.95 M).

To support and expand upon these results, we turned to wide angle X-ray diffraction. The rationale for this

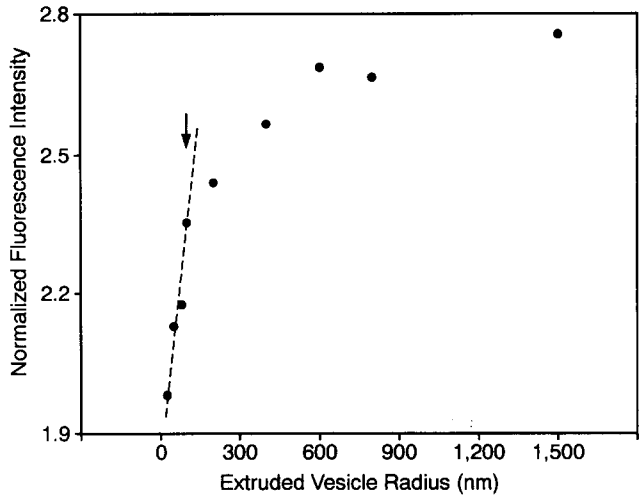

Fig. 1. Fluorescence intensity of DPH incorporated into vesicles of various sizes. Fluorescence intensity at 23°C was measured for a series of vesicles, ranging in size from the smallest (sonicated unilamellar vesicles) to the largest (multilamellar vesicles) with intermediate sizes provided by extrusion. Multilamellar vesicles were prepared by hydrating a stock solution of approx. 15 millimolar DPPC and 30 micromolar DPH in 150 mM NaCl, 10 mM Tris (pH 7.4) buffer. Aliquots of this stock solution were used to extrude vesicles through the following pore sizes: 50 nm, 80 nm, 100 nm, 200 nm, 400 nm, 600 nm and 800 nm. Sonicated vesicles were prepared from the same stock solution using a probe tip sonicator. Vesicles were maintained above their phase transition temperature until use. Fluorescence measurements were performed on a PTI deltascan spectrofluorometer operating in the single excitation mode. Samples for fluorescence measurements were prepared by 100-fold dilution into either Tris buffer or ethanol. In order to minimize any artifacts which might arise from vesicle size dependence of DPH aqueous or bilayer partition coefficients, the absolute fluorescence intensity measured in Tris buffer was normalized to the absolute fluorescence intensity of samples dissolved in ethanol. Excitation was at 350 nm with the emission monitored between 375 nm and 600 nm. The vesicle size dependence of these normalized fluorescence intensities measured by integrated peak areas and as peak heights of the three prominent transitions in the fluorescence spectrum (403, 428 and 451 nm) is displayed. The discontinuity at 100 nm (see arrow) likely corresponds with the transition from unilamellarity (< 100 nm) to multilamellarity (> 100 nm) [33].

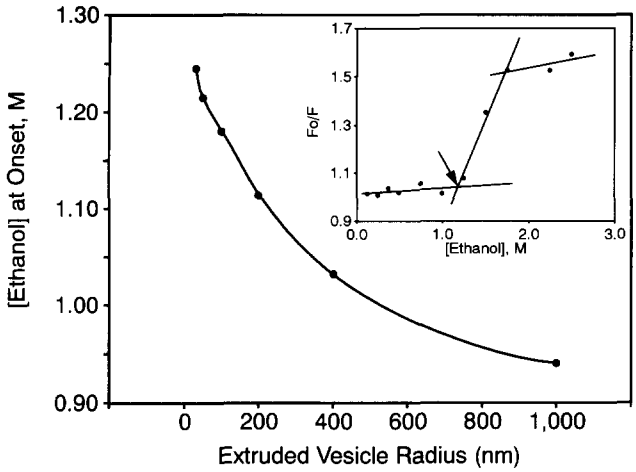

Fig. 2. The ethanol concentration (M) required to induce the onset of interdigitation in DPPC vesicles of various sizes following 1.0 h incubations at 23°C. The onset ethanol concentration was determined in separate experiments for each sized population of vesicles labeled with DPH A pseudo Stern-Volmer plot was constructed in which the ratio F_0/F (where F_0 is the fluorescence intensity in the absence of ethanol and F the fluorescence intensity in the presence of ethanol) was plotted against ethanol concentration (M). These plots which are sigmoidal in nature (see inset for 100 nm vesicles) were fitted with straight lines and the lowest ethanol concentration corresponding to the first inflection taken as the onset concentration (see text). Differences in fit paridigms resulted in small variations in onset ethanol concentrations which are contained numerically within the data points shown. Initial lipid concentrations were typically 20 mM, but were diluted to 0.15 mM with the specified ethanol solutions prior to measurements. Variation of the initial lipid concentrations over a wide range (0.15–50 mM) did not effect results. When these experiments were conducted at 50°C no quenching of fluorescence was observed consistent with the inability of DPPC to interdigitate in the liquid crystalline phase. Similarly, EPC MLVs and SUVs did not interdigitate at room temperature.

choice concerned experiments described by Braganza and Worcester [25] who found that the peak of the wide angle X-ray scattering (WAXS) of gel-state DPPC which occurs at 4.2 Å was shifted to 4.12 Å when the interdigitated state was induced by high pressure. The 4.12–4.2 Å peak results from correlations in the distances between the carbon atoms in the acyl chains; smaller values correspond to more tightly packed chains. Although in multilamellar systems the assignment of the interdigitated phase can be made by an electron density reconstruction derived from small angle diffraction, in unilamellar vesicles the lack of a periodic structure makes such reconstruction problematic. Wide angle scattering, by contrast, can be used to detect interdigitation in both systems because it arises from correlations within bilayers as opposed to between bilayers and thus is insensitive to lamellarity. Fig. 3 shows that in the presence of ethanol, interdigitation as judged by WAXS was complete in MLV systems at 1.0 M concentrations but could only be detected in SUVs systems at concentrations significantly above this value. These experiments, consistent with the fluorescence experiments, indicate that the bilayer to interdigitated bilayer transition in DPPC is sensitive to vesicle radius of curvature. Note that in the absence of ethanol the WAXS peaks for SUVs were broader than is typical for larger vesicles. This suggests an inability of the acyl chains to pack efficiently due to the high bilayer curvature in SUVs.

In the course of our investigations, we noted that suspensions of liposomes up to about 200 nm became turbid, even viscous, at concentrations of ethanol required to induce interdigitation. Freeze fracture microscopy (Fig. 4) revealed that in 2.0 M ethanol 100 nm

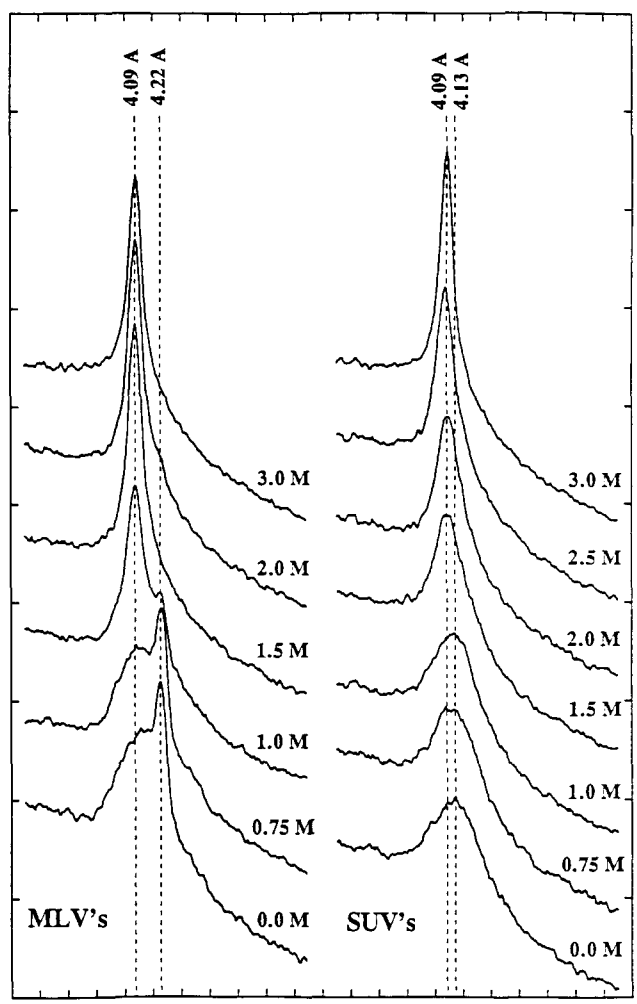

Fig. 3. Wide angle X-ray diffraction patterns recorded at 25.0°C of MLVs (left) and SUVs (right) exposed to various concentrations of ethanol (indicated in molar concentration on each curve). The shift in the diffraction peak from a spacing of 4.22 Å to 4.09 Å suggests a bilayer to interdigitated bilayer transition between 0.75 to 1.0 M ethanol for MLVS. The small peak at 4.22 Å still present at 1.0 M ethanol likely arises from a small population of vesicles < 200 nm, which are not fully interdigitated (see Fig. 2). In these experiments, sample heterogenity was not evident in populations of SUVs. For SUVs in the presence of 1.0 M ethanol or less, a single broad peak at 4.13 Å is observed. At 1.5 M ethanol, the diffraction peak begins to sharpen and shift to 4.09 Å. At 3.0 M ethanol, the peaks from MLVS and SUVs are equivalent.

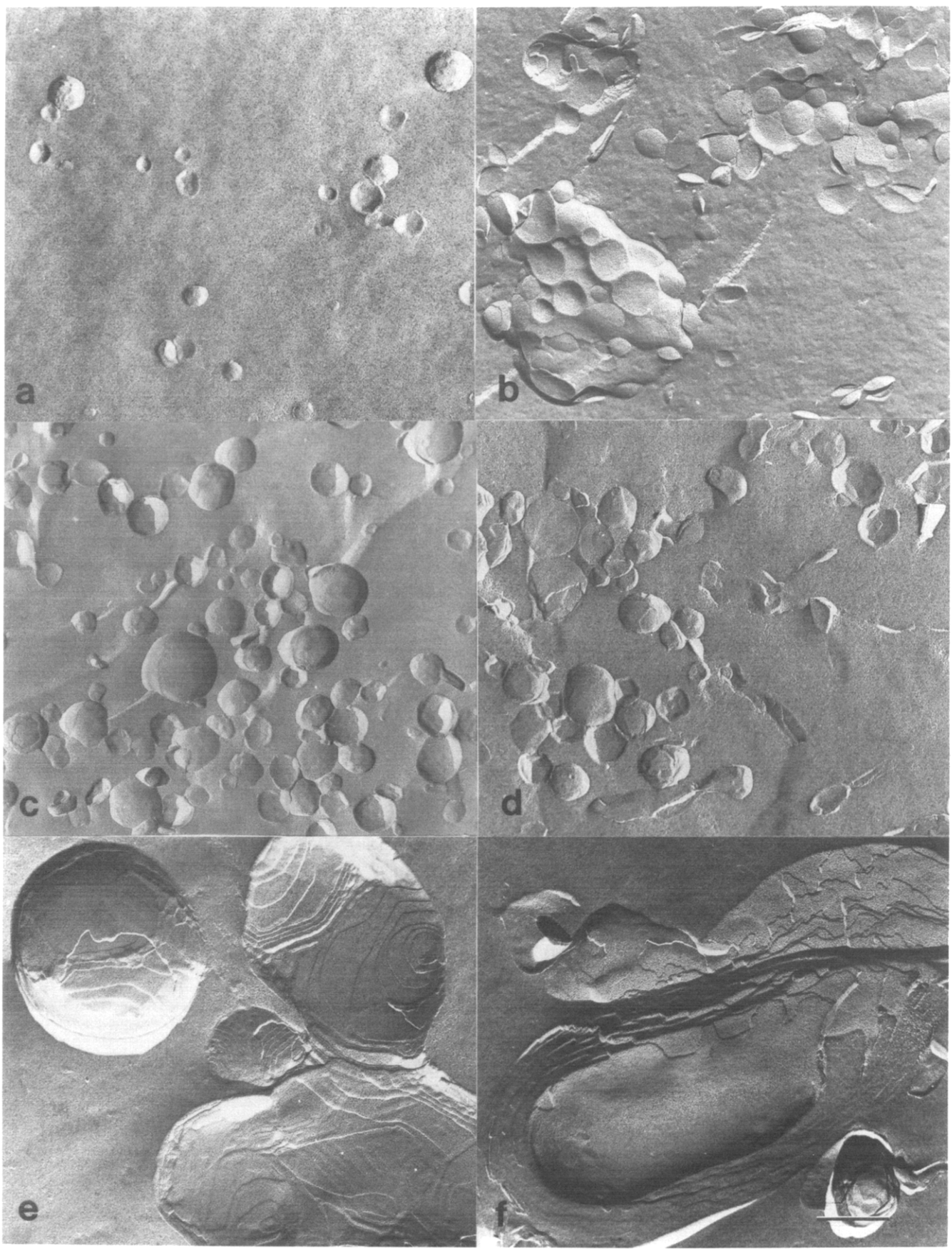

Fig. 4. For legend see p. 253.

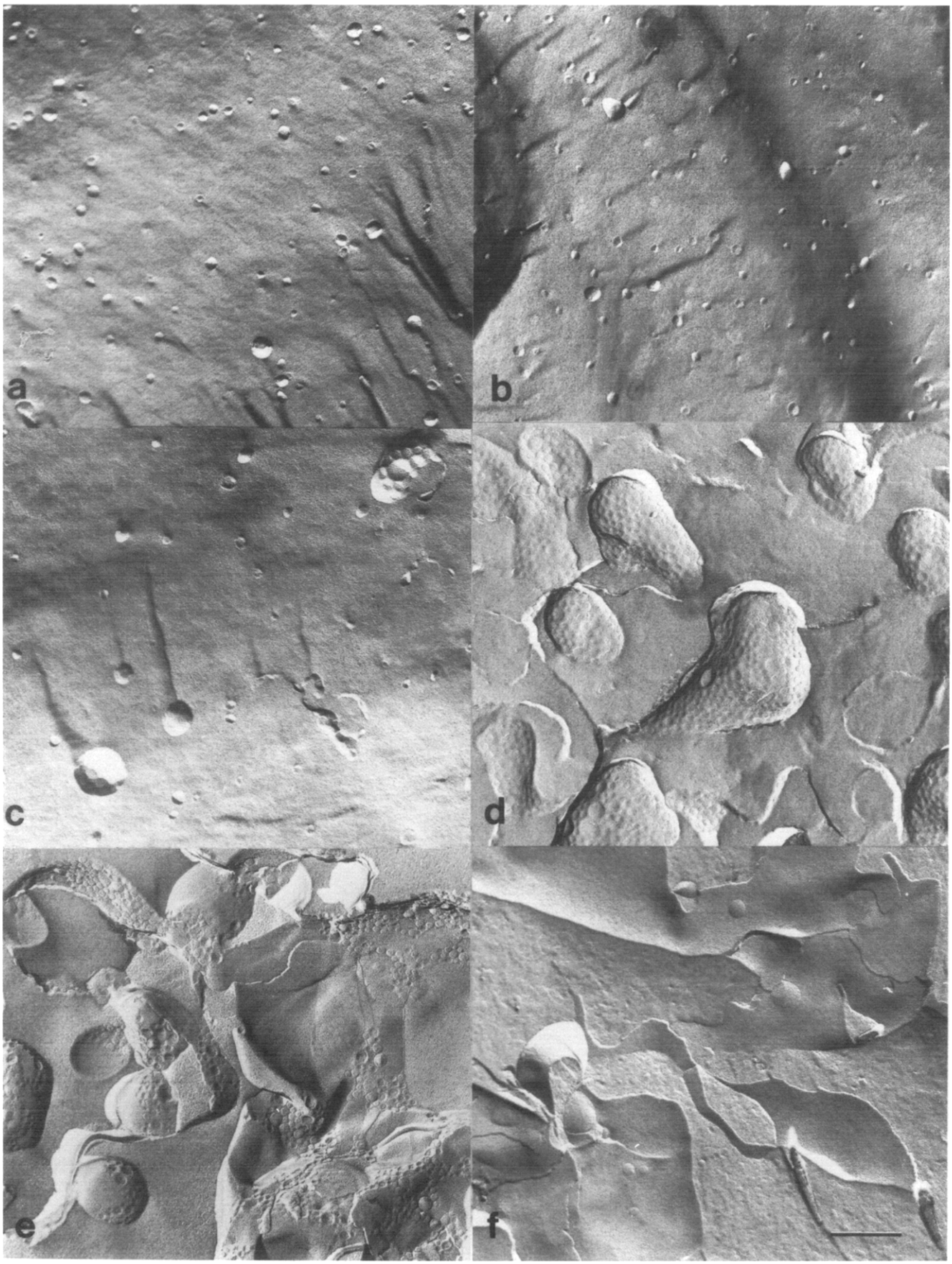

Fig. 5. For legend see p. 253.

extruded LUVETs (which in the absence of ethanol exhibit multifaceted fracture faces, a consequence of curvature imposed packing constraints) coalesced into aggregates of fused vesicles. Similar behavior was observed for 50 nm vesicles (data not shown). Little change, however, was observed for 200 nm vesicles exposed to 2.0 M ethanol. And as observed by freeze fracture, the sole effect of ethanol upon MLVs was an obliteration of the P'_β structure and an increase in cross fracturing, as would be expected for interdigitated vesicles [26]. We further employed freeze-fracture microscopy to systematically determine the morphological changes in DPPC vesicles as a function of ethanol concentration (Fig. 5). No differences were noted between SUVs in 1.0 M ethanol and those without ethanol present (Fig. 5a and b). In the presence of 1.5 M ethanol, however, a concentration shown by both the X-ray diffraction and fluorescence measurements to correlate with the onset of the interdigitated phase, small clusters of aggregated or fused vesicles were apparent (Fig. 5c). At 2.0 M ethanol massive coalescence of SUVs to form large sheets of lipid were noted. These sheets had dimpled surfaces, presumably remnants of the SUVs from which they arose (Fig. 5d). Such structures appeared somewhat stable for they persisted following the removal of ethanol through washing by centrifugation (Fig. 5e), a procedure shown by DPH measurements to reverse the interdigitated phase. In 2.5 M ethanol SUVs rapidly coalesced into extended smooth sheets that took on a gel like consistency (Fig. 5f). Small angle X-ray diffraction of these dispersions indicated a multilamellar lattice with a 48.8 Å repeat, or long spacing (Fig. 6). This spacing is identical to that found for MLVs interdigitated in the presence of 2.5 M ethanol. This can be contrasted to the spacing on the order of 60 Å for the noninterdigitated gel phase in DPPC [2].

Since the product of the fusion event was found to be a highly planar interdigitated bilayer, it seemed clear that the size dependence we were observing was based on the fact that the geometry of small vesicles could not accommodate interdigitation. But because the fusion of highly curved vesicles into interdigitated sheets occurred so rapidly, we could not easily determine whether a change in vesicle geometry preceded the fusion event. To address this we studied by freeze fracture DPPC liposomes of various sizes in 95 percent glycerol. This concentration of glycerol is known to induce DPPC interdigitation [3], and we believed its viscosity would decelerate the rate of liposome coalescence enough that the morphology of individual liposomes could be examined. As shown in Fig. 7, SUVs, which appeared primarily as individual liposomes, not

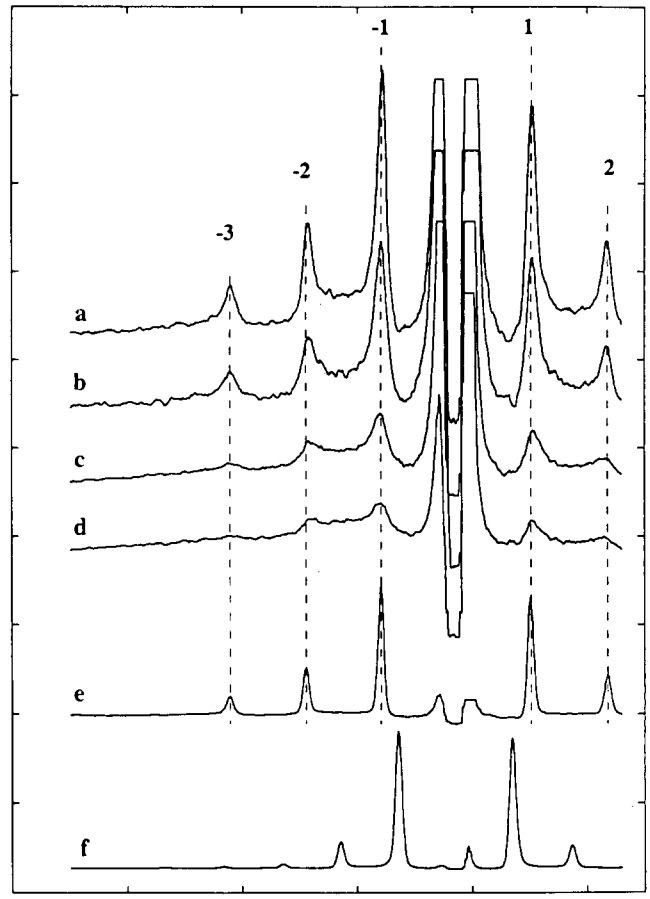

Fig. 6. (a–d) Small angle X-ray diffraction patterns resulting from the extended lipid sheets formed by exposing (a) 300 mM, (b) 150 mM, (c) 50 mM and (d) 20 mM SUV dispersions to 2.5 M ethanol for greater than 1 h (see Fig. 4). Measurements were made at room temperature. All concentrations of lipid yielded interdigitated sheets with $d = 48.8$ Å. Dashed lines indicate the expected position of diffraction peaks with this spacing, (e) Interdigitated DPPC MLVS in 2.5 M ethanol with $d = 48.8$ Å, (f) DPPC MLVS in the absence of ethanol ($d = 63$ Å).

Fig. 4. Freeze-fracture electron micrographs of vesicles extruded through various nucleopore filters and exposed to 2.0 M ethanol. All dispersions contained 20 mM lipid and were quenched from 20°C 1.0 h following incubations. (a) 100 nm extruded LUVETs, (b) 100 nm extruded LUVETs and 2.0 M ethanol. (c) 200 nm extruded LUVETs, (d) 200 nm extruded LUVETs and 2.0 M ethanol, (e) MLVs, (f) MLVs and 2.0 M ethanol. Bar = 200 nm.

Fig. 5. Freeze-fracture electron micrographs revealing morphology of SUVs following exposure to (a) 0.0 M, (b) 1.0 M, (c) 1.5 M, (d) 2.0 M and (f) 2.5 M ethanol. All dispersions contained 20 mM lipid and were quenched from 20°C following incubations. Note that vesicle coalescence only occurred at ethanol concentrations able to induce interdigitation (> 1.0 M; see text). Coalescence was irrevesible and evident even when ethanol was removed by multiple dilutions and centrifugations (e). In 2.0 M ethanol this coalescence occurred slowly but within 24 hours evolved into the sheets that were immediately evident in 2.5 M ethanol. Bar = 200 nm.

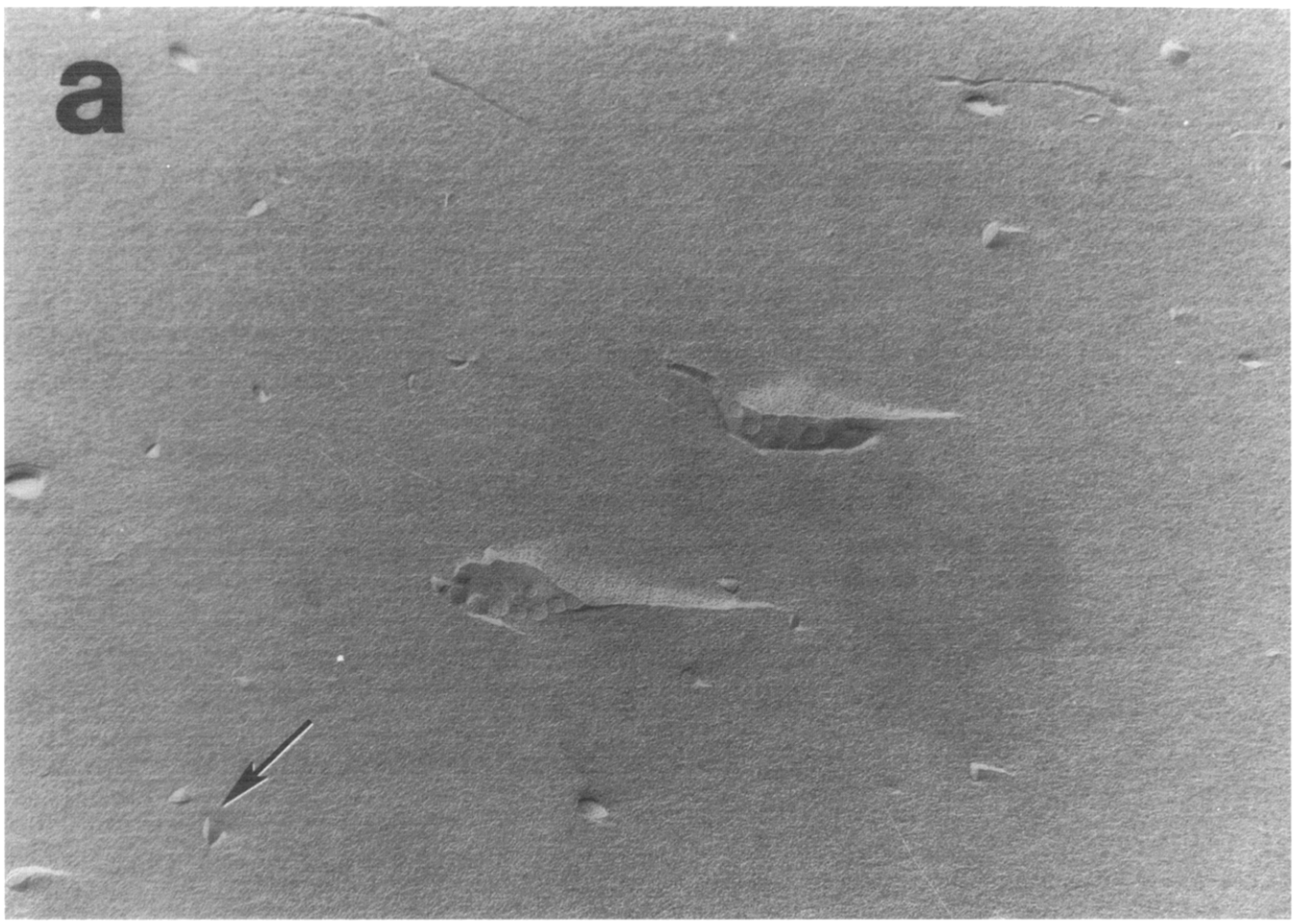

Fig. 7. Freeze-fracture electron micrographs of (a) DPPC SUVs, (b) 100 nm extruded LUVETs and (c) 400 nm extruded LUVETs in 95 percent glycerol (v/v). After examination of numerous micrographs, we found that only vesicles (50 percent shadowed) above 110 nm in diameter were spherical. Below this size liposomes possessed two to three faces with sharp contacting edges (noted by arrows). Liposomes and glycerol were mixed at 50°C and the resulting suspension cooled to room temperature and then frozen and fractured using the Balzer knife attachment. The high concentration of glycerol afforded cryoprotection. Bar = 200 nm.

aggregates, took on an ellipsoidal shape. Similarly 100 nm extruded LUVETs also appeared ellipsoidal. Unlike the multifaceted surfaces normally observed with small gel state DPPC liposomes (recall Fig. 4A) only two to three large faces were apparent. Presumably this change in geometry to an overall more planar bilayer occurred to allow acyl chain interdigitation. The ensuing rapid aggregation and fusion of these systems in less viscous ethanol solutions is not surprising since such surface morphology would produce hydrophobic exposure at the sharp edges where planar interdigitated faces meet. Note that 400 nm extruded LUVETs remained spherical in shape (Fig. 7c).

To more accurately quantitate the extent of lipid mixing resulting from the exposure of small lipid vesicles to ethanol, we employed resonance energy transfer (RET). In these studies vesicles containing both NBD-PE and rhodomine-PE were mixed with blank vesicles at a 1:10 ratio. Lipid mixing was determined by taking advantage of the fact that RET between probes is distance dependent and diminishes as the probe molecules mix with blank vesicles. Mixing was quantified by the use of a standard curve (see Materials and Methods) in which a 1:100 dilution of probe was considered representative of 100% lipid mixing. Only minimal mixing ($\sim$ 10%) was observed in vesicles 200 nm or greater at any ethanol concentration, consistant with freeze-fracture visualizations. Above concentrations of ethanol required to induce interdigitation (recall Figs. 2 and 3), lipid mixing in SUVs was evident and in fact was extensive at 1.75 M ethanol, reaching levels of 50 percent or greater. At higher concentrations of ethanol, the viscosity of the resulting gel made determinations difficult. In control experiments, we found that systems unable to interdigitate did not exhibit mixing. Thus, no lipid mixing was observed for a 20 mM suspension of egg PC SUVs in 2 M ethanol and less than 10% mixing occurred when 50 nm DPPC LUVETs were exposed to 2 M ethanol in the liquid crystalline state at 50°C.

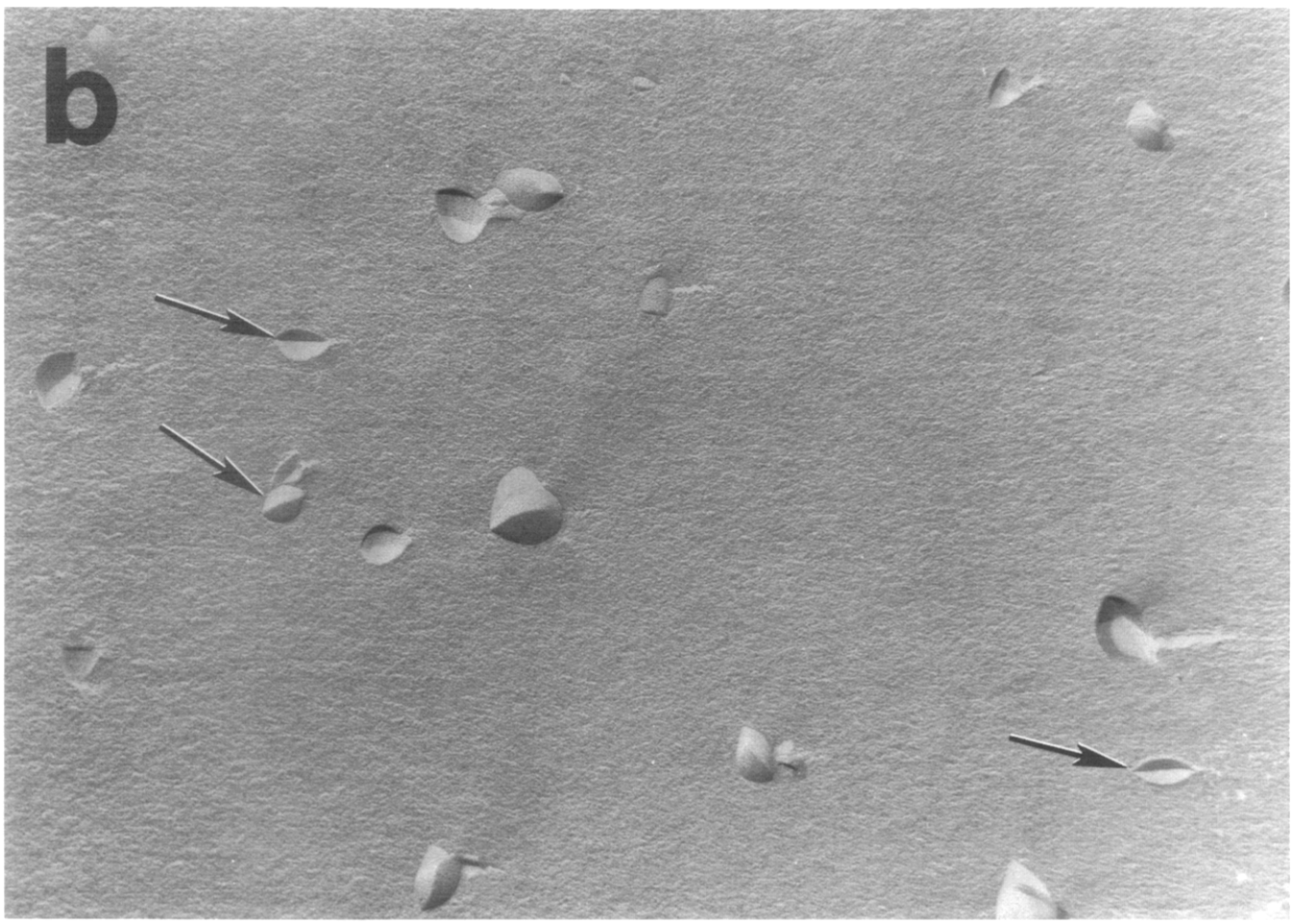

Fig. 7 (continued).

Employing an internal contents mixing assay, we found that for the most part lipid mixing between adjacent vesicles did not imply conserved mixing of aqueous phases. In these experiments two populations of SUVs, one containing ANTS and the other containing DPX in their aqueous phases were mixed at a 1:9 ratio and exposed to 2.5 M ethanol. Mixing of aqueous contents was detected by monitoring the decrease in ANTS fluorescence due to quenching by DPX (see Materials and Methods) and was found to be less than ten percent. In separate experiments both ANTS and DPX were encapsulated within the same SUVs and leakage as a function of ethanol concentration was monitored by an increase in ANTS fluorescence intensity after a 1.0 h exposure. Leakage did not occur at 1.0 M ethanol, a concentration unable to induce interdigitation or vesicle coalescence in SUVs, but did occur at higher concentrations. When exposed to 1.5 M or 2.0 M ethanol leakages of 25 and 49%, respectively, were detected. Thus, we conclude that concentrations of ethanol able to induce the interdigitated phase in SUVs do so by promoting vesicle coalescence and content leakage resulting in the formation of a viscous gel comprised of interdigitated lipid sheets.

Discussion

We have shown that the concentrations of ethanol required to induce interdigitation in DPPC systems increase with decreasing vesicle size. In fact, we found, as implied earlier, that ethanol induced interdigitation does not stably occur in intact vesicles below 100–200 nm in diameter at all [18,27]. Instead we report here that when exposed to ethanol these systems coalesce into extended interdigitated sheets which form the matrix of a viscous gel. These sheets can be fused into liposomes of high captured volume as discussed elsewhere [19]. Such liposomes may be useful in a variety of biomedical applications [28,29].

The present study was principally concerned with characterizing the size dependence and nature of ethanol induced interdigitation in DPPC vesicles. Both wide angle X-ray diffraction and fluorescence intensity measurements relying on phase dependent changes in

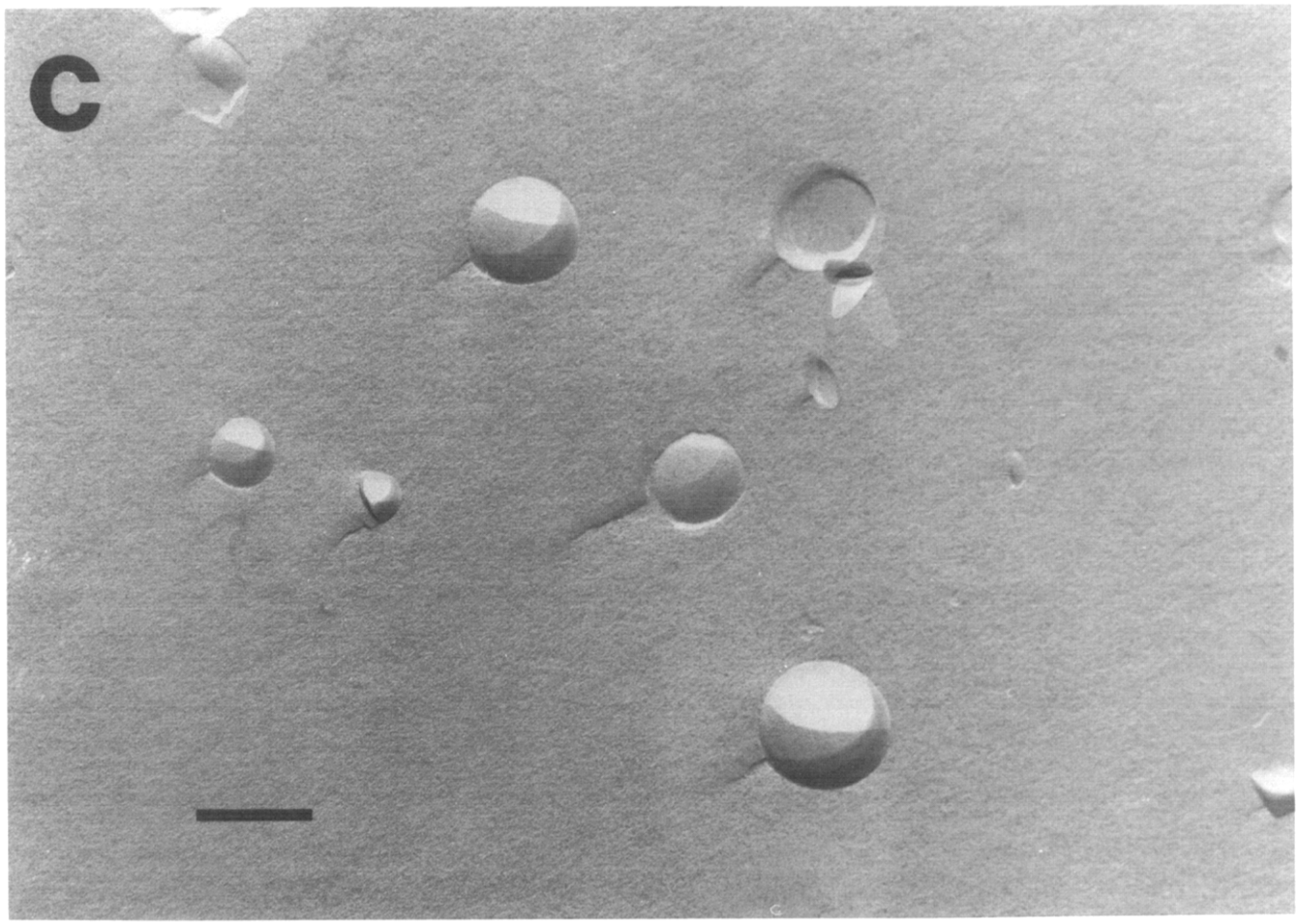

Fig. 7 (continued).

DPH orientation indicated that the onset of the interdigitated phase in SUVs occurred at ethanol concentrations 300 mM higher than those required to induce interdigitation in MLVs, suggesting temperature-alcohol phase diagrams [21] will vary as a function of DPPC vesicle size. At interdigitation inducing concentrations of ethanol vesicles on the order of 200 nm or smaller in diameter fused into extended sheets as visualized by freeze-fracture microscopy. Fusion involved extensive mixing of lipid as judged by RET techniques but not mixing of the internal contents of the contributing vesicles as determined by an ANTS-DPX assay. In the present study we relate fusion to the requirement of gel phase DPPC bilayers in ethanol to adopt the energentically favored interdigitated state. Bilayer curvature defined the concentration of ethanol necessary to induce interdigitation and became limiting when vesicle diameters were reduced to less than 200 nm forcing the fusion of such vesicles as a consequence of interdigitation. In fact it seems likely that interdigitation drove the fusion event. EPC SUVs which cannot interdigitate due to the unsaturated nature of their acyl chains, did not fuse in the presence of ethanol. Moreover, liquid crystalline phase DPPC SUVs, also incapable of interdigitation, did not fuse in the presence of ethanol.

In summary, we would point out that the process of interdigitation in an isolated vesicle requires a surface area approximating a locally planar bilayer. If this process is to occur at constant enclosed volume (i.e., without vesicle leakage) involving a small, highly curved, initially spherical vesicle, then the shape of the vesicle must change to accommodate a larger surface area to volume ratio. For particularly small vesicles, the shape change may be expected to introduce an energetically unfavorable curvature stress. The broadness of the X-ray diffraction peak at 4.1 Å arising from SUVs relative to that measured in MLVs is evidence of already pre-existing curvature stress. This curvature stress becomes vanishingly small as the size of the vesicle increases [30] and may be the mechanism mitigating against interdigitation in SUVs and similarly strained vesicles. Thus, corresponding higher concentrations of ethanol are required to induce the interdigitated phase in smaller DPPC vesicles and vesicle size must be accounted for in any thermodynamic treat-

ment of the L_{β} to L_{β_I} transition [31]. At concentrations of ethanol sufficiently high to force small vesicles into an interdigitated state, vesicle rupture and coalescence to form larger structures with lower mean curvature may be a release mechanism for the further induced curvature stress. We found that in glycerol, coalescence is in fact initiated by a change in vesicle morphology to produce a more planar bilayer. Presumably, this shape change increases the packing defects known to exist in saturated phosphatidylcholines below their gel to liquid crystalline phase transition [32]. Thus, greater exposure of the hydrocarbon portions of the bilayer to the aqueous phase occurs, particularly where the nascent highly planar surfaces meet (see Fig. 7a and b), driving the fusion event. We do not rule out the possibility that size related interdigitation dependent fusion events may be important in biological phenomena involving lipids such as DPPC and sphingomyelin which are capable of interdigitation under physiological conditions.

Acknowledgement

This work was supported by The Liposome Company, Inc., Princeton, NJ.

References

1 Slater, J.L. and Huang, C.H. (1988) Prog. Lipid. Res. 27, 325–359.
2 Simon, S.A. and McIntosh, T.J. (1984) Biochim. Biophys. Acta 773, 169–172.
3 McDaniel, R.V., McIntosh, T.J. and Simon, S.A. (1983) Biochim. Biophys. Acta 731, 97–108.
4 McIntosh, T.J., McDaniel, R.V. and Simon, S.A. (1983) Biochim. Biophys. Acta 731, 109–114.
5 Cunningham, B.A. and Lis, L.J. (1986) Biochim. Biophys. Acta 861, 237–242.
6 Wilkinson, D.A., Tirrell, D.A., Turels, A.B. and McIntosh, T.J. (1987) Biochim. Biophys. Acta 905, 447–453.
7 Ranck, J.L. and Tocanne, J.F. (1982) FEBS Lett. 143, 171–174.
8 Boggs, J.M. and Rangarai, G. (1985) Biochim. Biophys. Acta 816, 221–233.
9 Huang, C., Mason, J.T. and Levin, I.W. (1983) Biochemistry 22, 2775–2780.
10 Hui, S.W., Mason, J.T. and Huang, C. (1984) Biochemistry 23, 5570–5577.
11 Xu, H. and Huang, C. (1987) Biochemistry 26, 1036–1043.
12 Mattai, J., Sripoda, P.K. and Shipley, G.G. (1987) Biochemistry 26, 3287–3297.
13 Rucco, M.T., Siminovitch, D.J. and Griffin, R.G. (1985) Biochemistry 24, 2406–2411.
14 Mattai, J. and Shipley, G.G. (1986) Biochim. Biophys. Acta 859, 257–265.
15 Hui, S.W. and Huang, C. (1986) Biochemistry 25, 1330–1335.
16 Levin, I., Thompson, T.E., Barenholtz, Y. and Huang, C. (1985) Biochemistry 24, 6282–6287.
17 Maulik, P.P., Atkinson, D. and Shipley, G.G. (1986) Biophys. J. 50, 1071–1077.
18 Boni, L., Minchey, S., Perkins, W., Ahl, P., Tate, M., Gruner, S. and Janoff, A.S. (1991) Biophys. J. 503a.
19 Ahl, P.L., Boni, L.T., Perkins, W.P., Slater, J.L., Minchey, S.R., Taraschi, T.F. and Janoff, A.S. (1992) Biophys. J. 243a.
20 Weibel, E.R. and Bolender, R.B. (1973) In Principles and Techniques of Electron Microscopy (Hoy at M.A., ed.), Van Nostrord Reinhold Co., New York.
21 Nambi, P., Rowe, E.S. and McIntosh, T.J. (1988) Biochemistry 27, 9175–9182.
22 Ellens, H., Bentz, J. and Szoka, F. (1986) Biochemistry 25, 4141–4147.
23 Gruner, S.M., Lenk, R.P., Janoff, A.S. and Ostro, M.J. (1985) Biochemistry 24, 2833–2842.
24 Gruner, S.M., Milch, J.R. and Reynolds, G.T. (1982) Nucl. Instrum. Methods Phys. Res. 195, 287–297.
25 Braganza, L.F. and Worcester (1986) Biochemistry 25, 2591–2596.
26 Hui, S.W., Mason, J.T. and Huang, C. (1984) Biochemistry 23, 5570–5577.
27 Komatsu, H., Guy, P.T. and Rowe, E.S. (1991) Biophys. J. 502a.
28 Janoff, A.S., Minchey, S.R., Perkins, W.R., Boni, L.T., Seltzer, S.E., Adams, D.F. and Blau, M. (1991) Invest. Radiol. 26, 5167–5168.
29 Seltzer, S.E., Janoff, A.S., Blau, M., Adams, D.F., Minchey, S.R. and Boni, L.T. (1991) Invest. Radiol. 26, 5169–171.
30 Gruner, S.M. (1987) In Liposomes from Biophysics to Therapeutics (Ostro, M., ed.), pp. 39–72, Marcel Dekker, New York.
31 Rowe, E.S. and Cutrera, T.A. (1990) Biochemistry 29, 10398–10404.
32 Larrabee, A.L. (1979) Biochemistry 18, 3321.
33 Mayer, L.D., Hope, M.J. and Cullis, P.R. (1986) Biochim. Biophys. Acta 858, 161–168.